Quantitative 3D Evaluation of Myocardial Perfusion During Regadenoson Stress using Multidetector Computed Tomography

Victor Mor-Avi[1], Nadjia Kachenoura[1,2], Joseph A. Lodato[1], Sonal Chandra[1], Benjamin H. Freed[1], Barbara Newby[1], Roberto M. Lang[1], Amit R. Patel[1]

[1]University of Chicago, Department of Medicine, Chicago, Illinois, USA
[2]Inserm, U678, Laboratoire d'Imagerie Fonctionnelle, 75013, Paris, France

Abstract

We tested the hypothesis that quantitative 3D analysis of myocardial perfusion from MDCT images obtained during regadenoson stress would more accurately detect the presence of significant coronary artery disease (CAD) than the same analysis when performed on resting MDCT images. Fifty consecutive patients referred for CT coronary angiography (CTCA) underwent additional imaging with regadenoson (0.4mg, Astellas) using prospective gating (256-channel, Philips). Custom software was used to calculate for each myocardial segment an index of severity and extent of perfusion abnormality, Qh, which was compared to perfusion defects predicted by the presence and severity of coronary stenosis on CTCA. In segments supplied by arteries with luminal narrowing >50%, myocardial attenuation was slightly reduced compared to normally perfused segments at rest (91±21 vs. 93±26 HU, NS), and to a larger extent at stress (102±21 vs. 112±20 HU, p<0.05). In contrast, index Qh was significantly increased in these segments at rest (0.40±0.48 vs. 0.26±0.41, p<0.05) and reached a nearly 3-fold difference at stress (0.66±0.74 vs. 0.28±0.51, p<0.05). The addition of regadenoson improved the diagnosis of CAD, as reflected by an increase in sensitivity (from 0.57 to 0.91) and improvement in accuracy (0.65 to 0.77). In conclusion, quantitative 3D analysis of MDCT images allows objective detection of CAD, the accuracy of which is improved by regadenoson stress.

1. Introduction

It is well established that multidetector computed tomography (MDCT) is powerful in ruling out significant coronary artery disease (CAD) in patients with chest pain, due to its high negative predictive value, which is typically reported to be above 90% [1]. However, it has been shown that only patients with hemodynamically significant stenosis benefit from revascularization regardless of the degree of apparent luminal narrowing [2]. Accordingly, an increasing number of studies have been focusing on the potential of MDCT to assess myocardial perfusion in addition to coronary anatomy [3].

Several recent studies underscored the need for vasodilator stress in order to accurately detect stress-induced ischemia with MDCT imaging [4], and tested the feasibility of detecting perfusion abnormalities induced by adenosine stress [5-10]. Although regadenoson, a specific A2A receptor agonist with an improved side-effect profile, is increasingly used as a vasodilator during nuclear stress testing, very little is known about its ability to detect myocardial perfusion abnormalities using MDCT imaging. Furthermore, MDCT based evaluation of myocardial perfusion remains mostly subjective and qualitative. In addition, this methodology involves selected 2D slices, rather than 3D analysis that would take into account the entire myocardium, and requires manual adjustment of the contrast windows, both carrying the risk of missing small or less pronounced perfusion defects.

To address this issue, we developed a technique for quantitative volumetric analysis of myocardial perfusion from MDCT images and tested its ability to detect fixed perfusion abnormalities confirmed by resting SPECT [11]. Our present study was designed to test the feasibility of this quantitative 3D perfusion analysis of MDCT images obtained during regadenoson stress and test the hypothesis that this approach would more accurately reflect the presence of significant CAD than the same analysis performed on resting MDCT images.

2. Methods

We studied 50 patients (age: 54±11 years, 31 males, body mass index: 29.3±5.6 kg/m²) who underwent clinically indicated CTCA and an additional scan during vasodilator stress. Patients with contraindications to CTCA, including known allergies to iodine, renal dysfunction, inability to perform a 10 sec breath-hold, and contraindications to beta-blockers or regadenoson,

were excluded from the study. In addition, patients who had history of cardiothoracic surgery or pacemaker implantation were excluded.

Images were acquired using an MDCT system (256-channel iCT scanner, Philips). Imaging settings included: 270 ms gantry rotation time, slice thickness 0.625 mm and tube currents 600-1000 mA. Iodinated contrast agent was injected into a right antecubital vein and followed by a 20 ml chaser bolus.

Resting images were acquired according to a standard clinical CTCA protocol using prospective gating at a 75% phase of the cardiac cycle. Contrast doses varied between 65 and 90 ml, which were infused at rates of 5-6 ml/sec with tube voltages between 100 and 140 kV, depending on individual patient's characteristics. Resultant radiation dose for resting imaging was 5.9±3.3 mSv.

After resting imaging was performed, regadenoson (Astellas) was administered (0.4mg, i.v.) at least 15 min later to ensure contrast clearance. Regadenoson stress images were acquired 1 min later to ensure imaging during peak effect. Imaging settings included: tube voltage of 100 to 120 kV at 40% phase of the cardiac cycle, using prospective gating to minimize radiation exposure [12]. Patients received 55-90 ml of iodinated contrast agent at a rate of 4-6 ml/sec. The resultant radiation dose for stress imaging was 4.3±3.5 mSv.

CTCA reading was performed on the resting images by an experienced reader, whose interpretation of coronary anatomy included the determination of presence, location and extent of stenosis in percent of luminal narrowing. Narrowing >50% was considered as significant stenosis. In addition, the specific location of stenosis, when detected on CTCA, was used to determine which myocardial segments would be affected.

Myocardial perfusion was analyzed both at rest and during regadenoson stress using custom software for volumetric analysis described previously [11;12]. Briefly, following manual initialization of endo- and epicardial boundaries, the endo- and epicardial 3D surfaces were automatically estimated using the level-set technique [13]. The 3D region of interest confined between the endocardial and epicardial surfaces was identified as LV myocardium and divided into 17 3D wedge-shaped segments: 6 basal, 6 mid-ventricular, and 4 apical. Coronary arteries and contrast-filled inter-trabecular spaces were excluded from the myocardial segments and papillary muscles and trabeculae were excluded from the LV cavity by setting thresholds on the histograms of x-ray attenuation [11;12].

For each myocardial segment, mean x-ray attenuation value was measured in Hounsfeld units (HU). Then x-ray attenuation in all LV slices from base to apex was used to generate a bull's eye display of myocardial attenuation normalized by mean LV cavity attenuation [11]. Unlike our previous study of fixed perfusion defects [11], in which the bull's eyes displayed transmural attenuation, in this study we created bull's eyes of subendocardial attenuation, to optimize the visualization of stress-induced perfusion defects.

In addition, for each myocardial segment, a quantitative index of extent and severity of perfusion abnormality, Qh, was calculated from the histograms of x-ray attenuation (fig. 1) [11]. Briefly, this index is a mathematical product of the number of voxels with low attenuation in percent of the total volume of the segment (reflecting the extent of the defect) and the difference between the attenuation in these voxels and the previously determined normal attenuation in the same anatomic location (reflecting the severity of the defect).

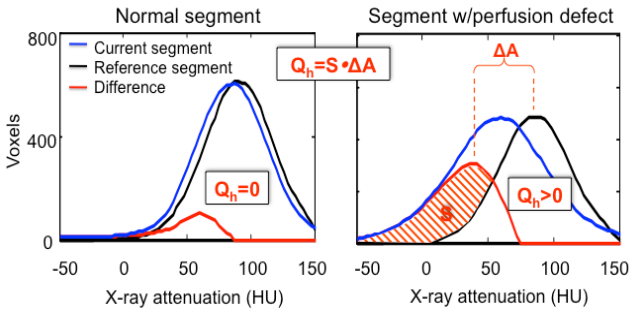

Figure 1. Quantification of extent and severity of myocardial hypoenhancement. Histograms of x-ray attenuation obtained in a segment with normal attenuation (left, blue line) and in a segment with a fixed perfusion defect on SPECT (right, blue line), shown with the adjusted reference histogram (black lines). While for the normal segment, the difference between the histogram and the adjusted reference (left, red line) overlapped completely with the reference, the abnormal segment was only partially overlapped with the adjusted reference (right, red line). The non-overlapping area, S, was used as a measure of the extent of hypoenhancement, and the distance between the peaks of the red and black curves, ΔA, was used as a measure of the severity of the defect.

Myocardial segments were then divided into two groups according to CTCA findings: segments supplied by coronary arteries with stenosis located proximally to the specific segment and causing >50% luminal narrowing on CTCA, and segments supplied by arteries without significant stenosis or with stenosis located distally to the segment. Both segmental myocardial x-ray attenuation and segmental values of index Qh were averaged separately for these two groups of segments, to determine to what extent these two indices differ between normally and abnormally perfused myocardium and test the hypothesis that Qh is superior to raw attenuation.

In addition, to determine the ability of the index Qh to classify segmental perfusion as normal or abnormal, ROC-derived threshold based classification of segments as normal or abnormal was compared to the CTCA

reference on a segment-by-segment, vascular territory and patient-by-patient basis.

These comparisons were performed separately for resting and stress images, in order to determine the added value of regadenoson stress for the detection of CAD.

3. Results

Three patients were excluded because of image artifacts. In the remaining 47 patients, CTCA depicted stenosis of >50% in 23 patients in 37/141 coronary arteries. With regadenoson, myocardial attenuation increased from 91±19 at rest to 110±19 HU ($p<0.05$), reflecting an increase in tissue blood flow. This is despite the decrease in LV cavity attenuation (437±144 to 310±73 HU, $p<0.05$), reflecting a decrease in contrast concentration as a result of increased cardiac output.

Figure 2 shows an example of MDCT images and bull's eyes of LV cavity normalized subendocardial x-ray attenuation, obtained at rest and peak regadenoson stress in a patient with significant CAD. The extent and severity of perfusion defect could be easily visualized in the bull's eye displays incorporating all LV slices from base to apex (right panels).

Overall, in segments supplied by obstructed arteries, myocardial attenuation was slightly reduced compared to normally perfused segments at rest (mean 91±21 vs. 93±26 HU, NS), and to a larger extent at peak regadenoson stress (mean 102±21 vs. 112±20 HU, $p<0.05$). In contrast, the mean value of index Qh was significantly increased in segments supplied by obstructed arteries at rest (0.40±0.48 vs. 0.26±0.41, $p<0.05$), reaching a nearly 3-fold difference at peak stress (0.66±0.74 vs. 0.28±0.51, $p<0.05$).

Figure 3 shows in a box-plot format the summary of both indices at rest and peak stress separately for the myocardial segments supplied by coronary arteries with and without significant stenosis. Compared to the raw x-ray attenuation, which had a considerable overlap between these two groups of segments both at rest and stress with little or no differences between median values (fig. 3, left), index Qh allowed better identification of abnormal perfusion at rest with median values of 0.24 vs. 0.07, and even more so at stress, with median values of 0.42 vs. 0.03 (fig. 3, right).

Table 1 shows the summary of results of the diagnostic accuracy analysis for this index on a segment-by-segment, coronary territory and patient basis both at rest and peak regadenoson stress. While on a segment-by-segment basis the sensitivity was relatively low, the specificity was quite good both at rest and stress (approximately 0.80). The transition to a territory basis resulted in a considerable improvement in sensitivity, especially at stress (0.73), without major changes in specificity. The patient-by-patient analysis resulted in the highest sensitivity, especially at stress (0.91), but at the expense of lower specificity, compared to the territory-by-territory analysis. Of note, the overall accuracy was in the mid 0.70s for all three analyses at stress. Importantly, all three analyses showed the incremental value of vasodilator stress, as reflected by higher values across the board in Table 1, compared to rest.

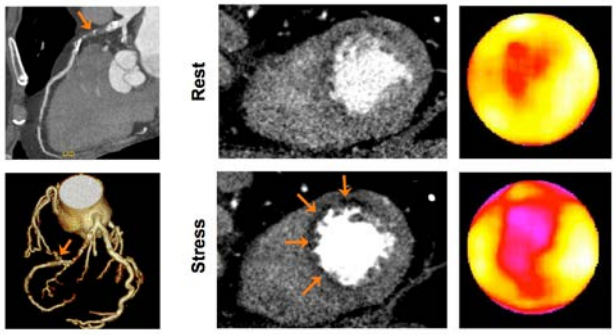

Figure 2. Example of images obtained at rest (top) and peak regadenoson stress in a patient with a fully occluded, calcified LAD artery (left top) showing retrograde filling via collaterals (left bottom). These images depict a mild resting perfusion defect in the anterior wall and the inter-ventricular septum (top center and right panels), which became more prominent during peak stress (bottom center and right panels).

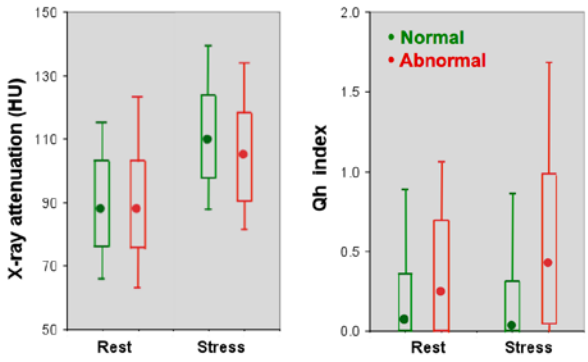

Figure 3. Box-plot summary of myocardial x-ray attenuation (left) and the 3D quantitative index Qh of severity and extent of perfusion abnormality (right) obtained at rest and peak stress separately for myocardial segments supplied by coronary arteries with (red) and without (green) significant stenosis.

		Sensitivity	Specificity	PPV	NPV	Accuracy
By segment	Rest	0.38	0.81	0.41	0.80	0.71
	Stress	0.55	0.79	0.45	0.85	0.73
By territory	Rest	0.43	0.85	0.52	0.80	0.74
	Stress	0.73	0.78	0.54	0.89	0.77
By patient	Rest	0.62	0.55	0.59	0.58	0.59
	Stress	0.91	0.58	0.68	0.88	0.74

Table 1. Diagnostic accuracy of the quantitative index of severity and extent of myocardial perfusion deficit derived by 3D analysis of cardiac CT images obtained at rest and during regadenoson stress, as determined by comparisons to CT coronary angiography findings in 47 patients. See text for details.

4. Discussion

We found that MDCT imaging during regadenoson stress was feasible and resulted in the majority of patients in images suitable for quantitative 3D analysis of stress perfusion, including the bull's eye displays depicting normalized subendocardial x-ray attenuation from ventricular base to apex in a single image. In addition, we evaluated a quantitative 3D index Qh, which was designed to reflect the relative size and severity of the perfusion defect, and is thus expected not to be as affected by the presence of the non-ischemic tissue within the same segment, as raw myocardial x-ray attenuation.

Our results indeed showed that myocardial segments affected by significant coronary stenosis had lower x-ray attenuation, but the variability in segmental attenuation caused by a variety of anatomical variables (e.g. body habitus) as well as technological factors (e.g. tube voltage, contrast infusion rates) did not always allow accurate detection of perfusion defects (fig. 3, left). The use of the segmental index of perfusion abnormality has circumvented many of these issues and allowed better differentiation between normally perfused and hypoperfused segments (fig. 3, right).

The use of this index resulted in good specificity and NPV on a segment and territory basis, indicating that perfusion defects, when detected, have an underlying anatomical cause. The relatively low sensitivity is a result of false negative detections, which may be explained by the fact that CTCA may not be the perfect reference, because it tends to overestimate the degree of stenosis. Importantly, the sensitivity and overall accuracy of this index considerably improved with regadenoson stress. This of course reflects the expected vasodilating effects of regadenoson, which is used to provoke ischemia, but it has not been demonstrated before for the combination of CT imaging and regadenoson.

One limitation of this study is the lack of direct perfusion assessment by an independent technique such as SPECT. While we agree that the study could be strengthened by SPECT data, such data is not available in the majority of patients referred for CTCA in our institution. Also, one might view as a limitation the use of CTCA as a reference for significant CAD. However, this choice was motivated by the desire to have a uniform reference across all study patients, which would not be the case had we used invasive angiography in patients in whom these data were available.

In summary, this is the first study to demonstrate that volumetric analysis of MDCT images obtained during regadenoson stress can detect hypoperfused myocardium. Although this methodology requires further validation, this study may have important implications on how MDCT stress perfusion imaging is performed and how the images are interpreted and analyzed.

Acknowledgements

This study was funded by a research grant from Astellas Global Development.

References

[1] Hulten EA, et al. Prognostic value of cardiac computed tomography angiography a systematic review and meta-analysis. J Am Coll Cardiol 2011; 57:1237-47.

[2] Tonino PA, et al. Angiographic versus functional severity of coronary artery stenoses in the FAME study fractional flow reserve versus angiography in multivessel evaluation. J Am Coll Cardiol 2010; 55:2816-21.

[3] Techasith T, Cury RC. Stress Myocardial CT perfusion. J Am Coll Cardiol Img 2011; 4:905-16.

[4] Kachenoura N, et al. Value of multidetector computed tomography evaluation of myocardial perfusion in the assessment of ischemic heart disease: comparison with nuclear perfusion imaging. Eur Radiol 2009; 19:1897-905.

[5] Kurata A, et al. Myocardial perfusion imaging using adenosine triphosphate stress multi-slice spiral computed tomography: alternative to stress myocardial perfusion scintigraphy. Circ J 2005; 69:550-7.

[6] George RT, et al. Multidetector computed tomography myocardial perfusion imaging during adenosine stress. J Am Coll Cardiol 2006; 48:153-60.

[7] Blankstein R, et al. Adenosine-induced stress myocardial perfusion imaging using dual-source cardiac computed tomography. J Am Coll Cardiol 2009; 54:1072-84.

[8] Cury RC, et al. Dipyridamole stress and rest myocardial perfusion by 64-detector row computed tomography in patients with suspected coronary artery disease. Am J Cardiol 2010; 106:310-5.

[9] Okada DR, et al. Direct comparison of rest and adenosine stress myocardial perfusion CT with rest and stress SPECT. J Nucl Cardiol 2010; 17:27-37.

[10] Rocha-Filho JA, et al. Incremental value of adenosine-induced stress myocardial perfusion imaging with dual-source CT at cardiac CT angiography. Radiology 2010; 254:410-9.

[11] Kachenoura N, et al. Volumetric quantification of myocardial perfusion using analysis of multi-detector computed tomography 3D datasets: comparison with nuclear perfusion imaging. Eur Radiol 2010; 20:337-47.

[12] Patel AR, et al. Detection of myocardial perfusion abnormalities using ultra-low radiation dose regadenoson stress multidetector computed tomography. J Cardiovasc Comput Tomogr 2011; 5:247-54.

[13] Corsi C, et al. Volumetric quantification of global and regional left ventricular function from real-time three-dimensional echocardiographic images. Circulation 2005; 112:1161-70.

Address for correspondence.

Victor Mor-Avi
University of Chicago Medical Center MC5084
5841 S. Maryland Ave., Chicago, IL 60637, U.S.A.
vmoravi@bsd.uchicago.edu